ChemComm

Cite this: *Chem. Commun.*, 2012, **48**, 10325–10327

www.rsc.org/chemcomm

COMMUNICATION

Design, synthesis and evaluation of small molecule reactive oxygen species generators as selective *Mycobacterium tuberculosis* inhibitors†

Allimuthu T. Dharmaraja,[a] Mallika Alvala,[b] Dharmarajan Sriram,[b] Perumal Yogeeswari[b] and Harinath Chakrapani*[a]

Received 24th July 2012, Accepted 20th August 2012
DOI: 10.1039/c2cc35343a

Here, we report 5-hydroxy-1,2,3,4,4*a*,9*a*-hexahydro-1,4-ethano-9,10-anthraquinone (13), a small molecule generating reactive oxygen species (ROS) in pH 7.4 buffer under ambient aerobic conditions that has selective and potent *Mycobacterium tuberculosis* growth inhibitory activity.

Tuberculosis (TB) remains a leading cause of morbidity and mortality in much of the world. *Mycobacterium tuberculosis* (*Mtb*), the etiological agent of this infectious disease, is a highly adaptive pathogen and an extremely difficult pathogen to kill. The alarming rise in co-infection with HIV as well as extensively drug resistant (XDR) and multi-drug resistant (MDR) strains[1] necessitates new chemotherapeutic strategies.[2] Maintenance of redox homeostasis is integral to the sustenance of metabolic processes and mycobacterial persistence. Any significant alterations in oxidative or reductive species might cause breakdown of this balance and lead to cell death.[3] For example, elevated levels of reactive oxygen species (ROS) such as superoxide $O_2^{-\bullet}$, hydrogen peroxide H_2O_2 and hydroxyl radical $^{\bullet}OH$ can cause irreparable damage to biomacromolecules including DNA leading to oxidative stress and might severely affect *Mtb* survival (Scheme 1).[4] A growing body of evidence points to normal human cells' ability to better tolerate alterations in redox homeostasis in comparison with cancer cells[5,6] and forms the basis of an emerging paradigm for new redox-directed cancer chemotherapeutics.[7] Thus, small molecules capable of perturbing mycobacterial redox homeostasis through generation of ROS might have selective *Mtb* growth inhibitory potential.[4]

2,3-Dihydro-1,4-benzoquinones (**A**) were considered as potential ROS generators (Scheme 2). Conversion of **A** to its tautomer 1,4-dihydroxyarene (**B**) might occur at physiological pH; the diol **B** can undergo aerobic oxidation to give **C** with concomitant production of $O_2^{-\bullet}$ and H_2O_2.[8] Variation of ring size "*n*" and functional groups X and Y could perturb keto–enol equilibria and as a consequence, ROS yields, allowing us to study the effects of varying ROS levels on *Mtb* growth inhibitory activity. Finally, 1,4-quinones such as **C** are candidates for bioreduction to regenerate **B**, which is capable of generating ROS.

In order to test our hypothesis, 2,3-dihydro-1,4-benzoquinones **1–12** were synthesized (ESI†) from commercially available starting materials by a [4 + 2] cycloaddition between a quinone and appropriate equivalents of a 1,3-diene (Fig. 1).

The ability of **1–12** to generate $O_2^{-\bullet}$ (Fig. 2a) and H_2O_2 (Fig. 2b) under ambient aerobic conditions in pH 7.4 buffer was estimated using reported assays.[9,10] The juglone derivative **4** generated the highest levels of ROS amongst **1–12**. Based on this result, we prepared a closely related analogue **13** by hydrogenation of **4** (Fig. 1). This compound was found to be superior to **4** in ROS generation for 30 min (Fig. 2a and b).

Anti-microbial effects of ROS are primarily mediated through induction of DNA damage.[4] Fe(II)-mediated nuclease activity of **1–13** was estimated using a pBR322 supercoiled plasmid cleavage assay and nick induction was observed in nearly all compounds tested (Fig. 2c). The compound's nuclease activity correlated well with its ROS generating ability, indicating that the observed DNA damaging effects were ROS-mediated (Pearson's correlation coefficient $R = 0.9475$, P-value < 0.0001, Fig. S2, ESI†).

In order to test our hypothesis that ROS generators can inhibit *Mtb* growth, a reported assay was used to determine minimum inhibitory concentrations (MICs) for **1–13** against *Mycobacterium tuberculosis* $H_{37}R_v$ (Table 1, entries 1–13).[11] Amongst these, four compounds: **3**, **4**, **6** and **13** were found to be good *Mtb* growth inhibitors with MICs < 10 μg mL^{-1}. Compounds **5** and **12** did not show any detectable inhibitory activity at 100 μg mL^{-1} (Table 1, entries 5 and 12). MIC of the best ROS generator **13** was superior to those of clinically used first-line TB drugs ethambutol and pyrazinamide (Table 1, entries 16–17) and presents opportunities for further development as a TB drug candidate.

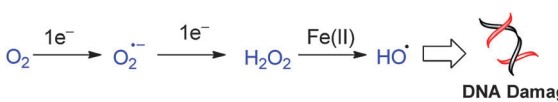

Scheme 1 Reactive oxygen species (ROS) generated through reduction of oxygen can damage biomacromolecules including DNA.

[a] *Department of Chemistry, Indian Institute of Science Education and Research (IISER) Pune, Pune 411 008, Maharashtra, India. E-mail: harinath@iiserpune.ac.in; Fax: +91-20-2589-9790; Tel: +91-20-2590-8090*
[b] *Department of Pharmacy, Birla Institute of Technology & Science Pilani, Hyderabad Campus, Jawahar Nagar, Hyderabad 500 078, India*

† Electronic supplementary information (ESI) available: Compound characterization data and assay procedures with relevant plots. CCDC 893408. For ESI and crystallographic data in CIF or other electronic format see DOI: 10.1039/c2cc35343a

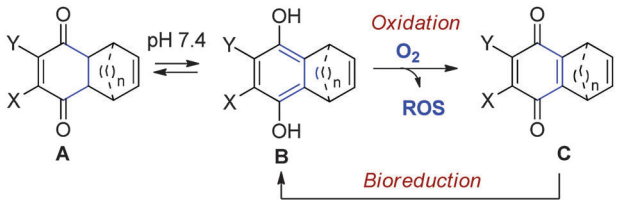

Scheme 2 Design of compounds that can perturb redox homeostasis by generating ROS.

Upon incubation of **13** at pH 7.4, HPLC analysis showed complete disappearance of **13** with concomitant formation of **14** at comparable rates in a nearly quantitative HPLC yield (Fig. 3a and b).[12] A first order increase of H_2O_2 for 12 h was observed with a maximal H_2O_2 yield of 72% (Fig. 3c). These results are consistent with a tentative mechanism based on enolization of 2,3-dihydro-1,4-naphthoquinones to produce a 1,4-diolate followed by reaction with oxygen to sequentially produce $O_2^{-\bullet}$ and H_2O_2 (Scheme S1, ESI†).[13,14] The presence of a proximal hydroxyl group appeared to diminish carbonyl π-character (IR spectroscopy, Fig. S6, ESI†); and enhanced electronegativity on the carbonyl oxygen (computational analysis, Fig. S7, ESI†). Together, these structural effects, likely due to intramolecular H-bonding (Fig. S8, ESI†), could promote enolization of C-4 carbonyl of **4** (or **13**) leading to enhanced ROS generation by these juglone derivatives in comparison with other analogues without a proximal hydroxyl group including the benzylated derivatives **8** and **9** (Fig. 1).

Compound **14**, the exclusive organic product during incubation of **13** did not generate $O_2^{-\bullet}$ or H_2O_2 in aerobic buffer (Tables S1 and S3, ESI†) and neither did it induce significant DNA damage (Fig. 2c). An increased intracellular fluorescence in the DCFH-DA-based assay conducted in the presence of *Mycobacterium smegmatis* MC^2155 (*Msm*) was observed (Fig. S4, ESI†). A quinone with a reduction potential in the range of −0.7 to −1.1 V would be predicted to be a candidate for reduction by enzymes such as NADPH:cytochrome P450 reductase[15] and CV analysis of **14** gave a reduction potential of −0.94 V (Fig. S9, ESI†). Together, these data are consistent with a bioreductive mode of activation of **14** to produce oxidative species (Scheme 1). Quinone **14** inhibited *Mtb* growth with a MIC of 1.56 μg mL^{-1} (Table 1, entry 14) supporting our hypothesis that direct generation of ROS by **13** (Fig. 1) in conjunction with intracellular production of oxidative species by redox cycling by **14** could result in inhibition of *Mtb* growth (Scheme 2).

The ROS generator **13** was not a significant inhibitor (IC_{50} > 25 μM) of normal human kidney (HEK) cells (Fig. S10, ESI†). This result is consistent with anti-cancer oxidative stress inducers which have shown selective toxicity towards cancers but spared normal cells.[5,6] The lead compound **13** (at 100 μg mL^{-1}) did not significantly inhibit several fast-growing Gram-positive and Gram-negative bacterial strains tested (Table S8, ESI†). The microbe selectivity of **13** parallels that of an artemisinin–mycobactin drug conjugate which has shown high *Mtb* inhibitory potency.[17]

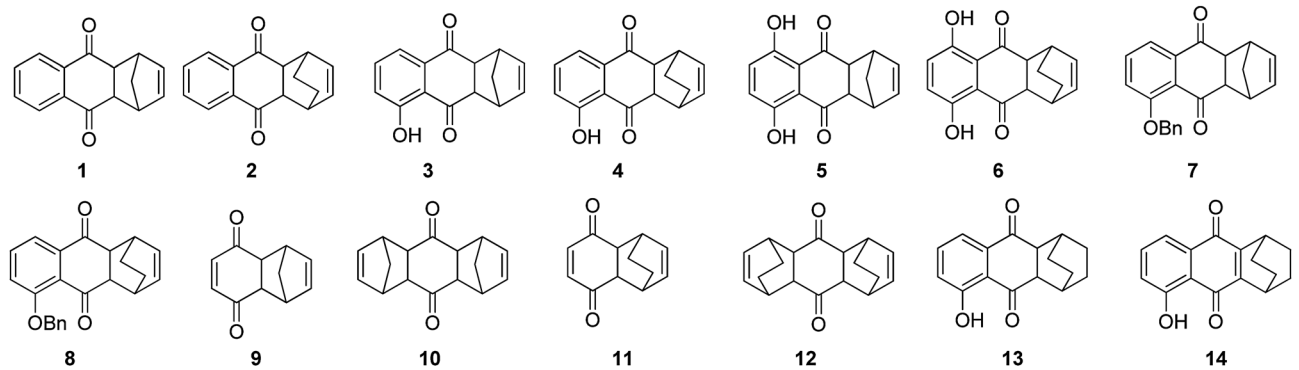

Fig. 1 Compounds **1–14**.

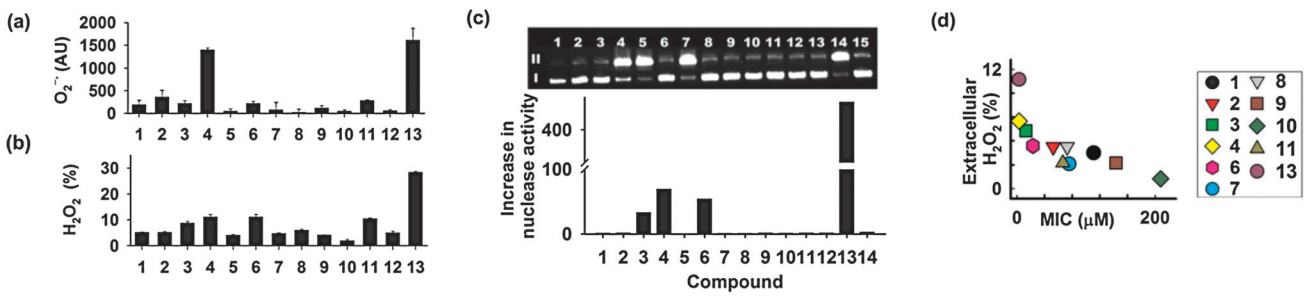

Fig. 2 (a) Superoxide ($O_2^{-\bullet}$) generated during incubation of **1–13** (5 μM) in pH 7.4 buffer at 37 °C for 30 min was estimated by a luminol-based chemiluminescence assay. Hypoxanthine/xanthine oxidase was used as a positive control in this assay. (b) H_2O_2 generated during incubation of **1–13** (5 μM) in pH 7.4 buffer at 37 °C for 30 min was estimated by a xylenol orange-based colorimetric assay; (c) nuclease activity of **1–14**: reaction mixtures (20 μL) contained 100 ng of form I DNA in pH 8.0 phosphate buffer (100 mM) and compound (50 μM) were incubated at 37 °C for 6 h: lane 1, untreated control; lane 2, **1**; lane 3, **2**; lane 4, **3**; lane 5, **4**; lane 6, **5**; lane 7, **6**; lane 8, **7**; lane 9, **8**; lane 10, **9**; lane 11, **10**; lane 12, **11**; lane 13, **12**; lane 14, **13**; lane 15, **14**. Nicked DNA is represented by II. A relative increase in nuclease activity is defined as the ratio of form II (cleaved) to form I (uncleaved) in comparison with untreated control (lane 1); (d) comparison of MICs determined against *Mycobacterium tuberculosis* and extracellular H_2O_2 yields during incubation of that compound with *Mycobacterium smegmatis* for 1 h and Spearman's correlation coefficient was found to be $\rho = -0.91$, *P*-value $< 10^{-5}$.

Table 1 Extracellular ROS generation, *Mycobacterium tuberculosis* growth inhibitory activity and calculated partition coefficients (clogPs)

Entry	Compd	MIC[a] (μg mL^{-1})	MIC (μM)	Extracellular H_2O_2[b] (%)	clogP[c]
1	**1**	25	111.0	3.6	2.43
2	**2**	12.5	52.4	4.2	2.99
3	**3**	3.13	13.0	5.8	2.76
4	**4**	0.76	3.0	6.8	3.32
5	**5**	>100	>350	1.9	2.72
6	**6**	6.25	23.1	4.3	3.28
7	**7**	25	75.6	2.5	4.29
8	**8**	25	72.5	4.2	4.85
9	**9**	25	143.5	2.6	0.43
10	**10**	50	208.0	1.0[d]	1.93
11	**11**	12.5	66.4	2.6	0.99
12	**12**	>100	>350	2.2[d]	3.04
13	**13**	0.76	3.0	11.0	3.81
14	**14**	1.56	6.1	3.8	4.52
15	Isoniazid	0.05	0.37	—	−0.67
16	Ethambutol	1.56	7.64	—	0.12
17	Pyrazinamide	6.25	50.8	—	−0.68

[a] Minimum inhibitory concentration (MIC) is the minimum concentration of the compound required to inhibit 99% of bacterial growth and was found against *Mycobacterium tuberculosis* $H_{37}R_v$ strain. [b] Extracellular H_2O_2 measured during incubation of **1–14** (50 μM) in the presence of *Msm* at 37 °C for 1 h estimated by an Amplex red-based fluorescence assay. [c] Calculated values using Chembiodraw Ultra. [d] Calculated based on 2 mol H_2O_2 from 1 mol of compound.

At the outset our goal was two-fold: one, to design, synthesize and study compounds that were capable of generating ROS; and two, to identify compounds with a range of ROS generation profiles by structural modifications to study the effects of varying ROS on *Mtb* growth. Having established that compounds **1–13** were ROS generators in buffer, we estimated ROS generated by **1–13** in the presence of cultured *Mycobacterium smegmatis* MC^2155 (*Msm*) and extracellular H_2O_2 was estimated using an Amplex Red-based fluorescence assay (Table 1). A good range of ROS in the presence of mycobacteria (1–11%) was observed with **13** being the best H_2O_2 generator (Table 1, entry 13). Statistical analysis between the compound's extracellular H_2O_2 yield in the aforementioned assay and the compound's measurable MIC against *Mtb* revealed a strong negative correlation (Fig. 2d) between these variables (Spearman's rank correlation coefficient $\rho = -0.91$, *P*-value $< 10^{-5}$). This result is indicative of ROS generating ability of the compound being important for inhibitory effects but without detailed mechanistic investigations, a conclusive connection cannot be established. However, previous studies show that the exquisite susceptibility of *Mtb* to isoniazid, a clinically used TB drug that in part acts through induction of oxidative stress, is attributable to inactivation of oxyR, a regulatory system that activates >20 anti-oxidant genes in response to ROS;[18] while oxyR is present in most actinobacteria, paradoxically, it is an inactive pseudogene in *Mtb* suggesting that a coherent response to induction of oxidative stress might be impaired.[19] Precursors of reactive species such as nitric oxide and sulfur dioxide have shown *Mtb* inhibitory activity.[11,16] Here, we demonstrate the feasibility of a tuberculosis drug design strategy based on compounds generating reactive oxygen species in order to perturb redox homeostasis.

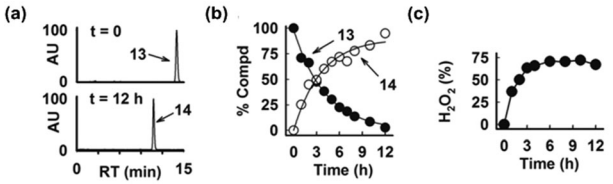

Fig. 3 (a) HPLC traces of incubation of **13** in pH 7.4 buffer for 12 h show complete conversion of **13** to **14**; (b) time courses of disappearance of **13** ($k_{13} = 0.24 \pm 0.01$ h^{-1}) and appearance of **14** (k_{14} was 0.28 ± 0.04 h^{-1}) based on HPLC analysis; (c) time course of H_2O_2 generated during incubation of **13** ($k_{HP} = 0.7$ h^{-1}) in pH 7.4 buffer.

This work was supported in part by Department of Biotechnology, India (BT/05/IYBA/2011). ATD acknowledges a research fellowship from Council for Scientific and Industrial Research (CSIR).

Notes and references

1 R. S. Wallis, W. Jakubiec, M. Mitton-Fry, L. Ladutko, S. Campbell, D. Paige, A. Silvia and P. F. Miller, *PLoS One*, 2012, **7**, e30479.
2 L. G. Dover and G. D. Coxon, *J. Med. Chem.*, 2011, **54**, 6157–6165.
3 A. Kumar, A. Farhana, L. Guidry, V. Saini, M. Hondalus and A. J. C. Steyn, *Expert Rev. Mol. Med.*, 2011, **13**, 1 (e39).
4 F. C. Fang, *Nat. Rev. Microbiol.*, 2004, **2**, 820–832.
5 L. Raj, T. Ide, A. U. Gurkar, M. Foley, M. Schenone, X. Li, N. J. Tolliday, T. R. Golub, S. A. Carr, A. F. Shamji, A. M. Stern, A. Mandinova, S. L. Schreiber and S. W. Lee, *Nature*, 2011, **475**, 231–234.
6 J. S. Bair, R. Palchaudhuri and P. J. Hergenrother, *J. Am. Chem. Soc.*, 2010, **132**, 5469–5478.
7 G. T. Wondrak, *Antioxid. Redox Signaling*, 2009, **11**, 3015–3069.
8 J. M. Campos-Martin, G. Blanco-Brieva and J. L. G. Fierro, *Angew. Chem., Int. Ed.*, 2006, **45**, 6962–6984.
9 H. Trung Pham, C. Marquetty, C. Pasquier and J. Hakim, *Anal. Biochem.*, 1984, **142**, 467–472.
10 C. Gay, J. Collins and J. M. Gebicki, *Anal. Biochem.*, 1999, **273**, 149–155.
11 S. R. Malwal, D. Sriram, P. Yogeeswari, V. B. Konkimalla and H. Chakrapani, *J. Med. Chem.*, 2012, **55**, 553–557.
12 J. A. Valderrama, O. Espinoza, M. F. Gonzalez, R. A. Tapia, J. A. Rodriguez, C. Theoduloz and G. Schmeda-Hirschmann, *Tetrahedron*, 2006, **62**, 2631–2638.
13 K. U. Ingold, T. Paul, M. J. Young and L. Doiron, *J. Am. Chem. Soc.*, 1997, **119**, 12364–12365.
14 J. Adamus, J. Gebicki, I. Ciebiada, E. Korczak and A. Denys, *J. Med. Chem.*, 1998, **41**, 2932–2933.
15 M. H. Livertoux, P. Lagrange and A. Minn, *Brain Res.*, 1996, **725**, 207–216.
16 R. Singh, U. Manjunatha, H. I. Boshoff, Y. H. Ha, P. Niyomrattanakit, R. Ledwidge, C. S. Dowd, I. Y. Lee, P. Kim, L. Zhang, S. Kang, T. H. Keller, J. Jiricek and C. E. Barry, 3rd, *Science*, 2008, **322**, 1392–1395.
17 M. J. Miller, A. J. Walz, H. Zhu, C. Wu, G. Moraski, U. Möllmann, E. M. Tristani, A. L. Crumbliss, M. T. Ferdig, L. Checkley, R. L. Edwards and H. I. Boshoff, *J. Am. Chem. Soc.*, 2011, **133**, 2076–2079.
18 C. D. den Hengst and M. J. Buttner, *Biochim. Biophys. Acta*, 2008, **1780**, 1201–1216.
19 E. Pagán-Ramos, S. S. Master, C. L. Pritchett, R. Reimschuessel, M. Trucksis, G. S. Timmins and V. Deretic, *J. Bacteriol.*, 2006, **188**, 2674–2680.